First publ. in: Journal of Biological Chemistry 286 (2011), 7, pp. 4991-5002

Neuroprotection by Minocycline Caused by Direct and Specific Scavenging of Peroxynitrite*

DOI 10.1074/jbc.M110.169565

Stefan Schildknecht[‡1], Regina Pape[‡], Nathalie Müller[§], Marta Robotta[¶], Andreas Marquardt[‖], Alexander Bürkle[§], Malte Drescher[¶], and Marcel Leist[‡]

From the Departments of [‡]In Vitro Toxicology and Biomedicine, and [§]Molecular Toxicology, Faculty of Biology, the [¶]Emmy Noether EPR Group, and the [‖]Mass Spectrometry Facility, Faculty of Chemistry, University of Konstanz, 78457 Konstanz, Germany

Minocycline prevents oxidative protein modifications and damage in disease models associated with inflammatory glial activation and oxidative stress. Although the drug has been assumed to act by preventing the up-regulation of proinflammatory enzymes, we probed here its direct chemical interaction with reactive oxygen species. The antibiotic did not react with superoxide or ·NO radicals, but peroxynitrite (PON) was scavenged in the range of ~1 μM minocycline and below. The interaction of pharmacologically relevant minocycline concentrations with PON was corroborated in several assay systems and significantly exceeded the efficacy of other antibiotics. Minocycline was degraded during the reaction with PON, and the resultant products lacked antioxidant properties. The antioxidant activity of minocycline extended to cellular systems, because it prevented neuronal mitochondrial DNA damage and glutathione depletion. Maintenance of neuronal viability under PON stress was shown to be solely dependent on direct chemical scavenging by minocycline. We chose α-synuclein (ASYN), known from Parkinsonian pathology as a biologically relevant target in chemical and cellular nitration reactions. Submicromolar concentrations of minocycline prevented tyrosine nitration of ASYN by PON. Mass spectrometric analysis revealed that minocycline impeded nitrations more effectively than methionine oxidations and dimerizations of ASYN, which are secondary reactions under PON stress. Thus, PON scavenging at low concentrations is a novel feature of minocycline and may help to explain its pharmacological activity.

Minocycline, a semisynthetic tetracycline derivative, has now been in clinical use for almost 40 years and is known for its excellent oral bioavailability and tissue distribution. Its efficient blood brain barrier passage (central nervous system/plasma distribution rate in the range of 0.3–0.6) allows central nervous system levels up to the micromolar range after repeated daily standard oral doses of 100–200 mg (1–3). In addition to its primary application as an antimicrobial agent, the use of minocycline has been considered in the field of neuroprotection (4, 5). Its tissue-protective properties have been demonstrated in animal models of stroke, amyotrophic lateral sclerosis, multiple sclerosis, and Parkinson, Alzheimer, and Huntington diseases (6–12).

Some direct neuroprotective actions of minocycline have been demonstrated *in vitro* (13, 14). Its beneficial *in vivo* activities have been suggested to be mainly based on its capacity to dampen glia activation and to reduce the tissue concentration of inflammatory mediators contributing to the degeneration process (11, 15–19). Accordingly, alterations of cell function by the antibiotic are best described for brain macrophages and microglial cells (20, 21). The majority of studies describe a reduced up-regulation of inflammatory components, such as surface markers, cytokines, or pro-inflammatory enzymes (22, 23). The reduced activity of enzymes such as nitric-oxide synthase or peroxidases is generally assumed to account for attenuated nitration of proteins caused by less peroxynitrite formation.

Apart from this hypothesis on indirect anti-inflammatory effects, relatively little information is available on the biochemical mode of action of minocycline. It has been argued that different targets are relevant in different settings, as suggested by largely varying effective concentrations of the drug (12, 16, 24, 25). Many studies observed an effect of the antibiotic on phosphorylation and hence the activation status of p38 MAPK, and a correlation of reduced p38 MAPK activation with the observed protective/anti-inflammatory effect was shown (12, 26). Other studies focused on a potential role of matrix metalloproteinase inhibition in the actions of minocycline (13, 27). However, a biochemically or pharmacologically defined target has not been characterized in any model system so far.

The difficulty of finding a protein-binding partner may be explained if minocycline acted by stoichiometric reaction with small molecules and thereby affected a multitude of processes indirectly. Such observations have been made earlier with other widely used drugs such as the analgesic acetaminophen, which has been demonstrated to act as selective scavenger of peroxynitrite (28). Because neurodegenerative diseases are always accompanied by inflammatory conditions (29), the potentially combined direct (on neurons) and indirect actions (prevention of detrimental inflammatory mediator synthesis) of minocycline would explain the good activity seen in animal models of disease. Reactive oxygen species generated in many cells under such conditions comprise H_2O_2, the hydroxyl radical (·OH), nitric oxide (·NO), superox-

* This work was supported by grants from the Doerenkamp-Zbinden foundation, the Land Baden-Württemberg, KoRS-CB, IRTG 1331, and the Deutsche Forschungsgemeinschaft.

[1] To whom correspondence should be addressed: University of Konstanz, P.O. Box M657, 78457 Konstanz, Germany. Fax: 49-7531-88-5039; Tel.: 49-7531-88-5053; E-mail: Stefan.Schildknecht@uni-konstanz.de.

ide ($O_2^{\cdot-}$), and peroxynitrite ($ONOO^-$). The latter anion or the decomposition products ($^{\cdot}NO_2$ and $^{\cdot}OH$) of its protonated form, respectively, can modify the structure and function of proteins and enzymes by nitration of tyrosine residues or by methionine sulfoxidation (30, 31). Prominent examples of signal transduction systems regulated by peroxynitrite are the NF-κB pathway (32) or mitogen-activated kinase cascades (26, 33). Moreover, disease-specific proteins such as the Parkinson disease-related protein α-synuclein are post-translationally modified by peroxynitrite and become more prone to form intracellular proteinaceous aggregates (34).

A potential role of minocycline as antioxidant has recently been suggested by studies showing that the compound can interfere with a battery of chemical radical generating systems or peroxynitrite (24, 35). However, these studies did not compare defined biologically relevant reactive oxygen species. Also, the effective concentrations of minocycline varied because of the different chemical assay systems used and often were 10–100 μM and higher. In contrast to this, we designed this study to investigate the direct interaction of minocycline with defined biological reactive oxygen species. In particular, we characterized its interaction with peroxynitrite in a pharmacologically relevant range. Our data show a specific interaction with this important intracellular signaling molecule and mediator of neurodegeneration in the submicromolar range. This first description of a molecularly defined target of minocycline may help to explain its broad effects in several different model systems.

EXPERIMENTAL PROCEDURES

Materials—Sin-1 (3-morpholinosydnonimine) (peroxynitrite generator), Spermine-NONOate (nitric oxide donor), and authentic peroxynitrite (PON)[2] were purchased from Cayman Chemicals (Ann Arbor, MI). Dihydrorhodamine 123 (DHR 123) and TEMPONE-H were from Molecular Probes (Carlsbad, CA), and L-012 was from Wako (Neuss, Germany). Wild type α-synuclein (ASYN), minocycline, tetracycline, gentamicin, rifampicin, ascorbic acid, uric acid, copper zinc-superoxide dismutase, KO_2, and AAPH (2,2′-azobis[2-methyl-propionamidine] dihydrochloride, and xanthine oxidase were from Sigma, and 4-dimethylaminophenol was from Koehler Chemie (Bensheim, Germany). Sin-1 and Spermine-NONOate solutions were prepared freshly before each experiment. Photometric determinations of PON stock concentrations were performed routinely (λ_{max}, 302 nm; ϵ, 1670 liter mol^{-1} cm^{-1}). PON was diluted in 0.3 M NaOH. When PON was used, an equal amount of equimolar HCl was added to the respective sample. In cell-free experiments, PON (in NaOH) and the corresponding volume of equimolar HCl were added carefully as separate droplets in the inner ring of a reaction tube, closed, and vortexed instantaneously and rigorously.

Radical Detection—The interaction between minocycline and PON was monitored by the oxidation of DHR 123 (1 μM) or by the luminol derivate L-012 (100 μM) in 10 mM potassium phosphate buffer, pH 7.4, containing desferoxamine (100 μM, to prevent Fenton chemistry reactions), if not otherwise indicated. The radical generating systems were incubated with the test compounds for 5 min at 37 °C before the radical detection dyes DHR 123 or L-012 were added and incubated for 15 min. Both dyes were chosen, because they are relatively selective for steady state PON levels in the submicromolar range. DHR 123 fluorescence (λ_{ex} = 485 nm, λ_{em} = 538 nm) as well as L-012 luminescence were detected in 96-well plates using a TECAN Infinite M200 reader.

$^{\cdot}NO$ Detection—Interaction between $^{\cdot}NO$ and minocycline was investigated by the use of the $^{\cdot}NO$-releasing compound Spermine-NONOate (10 μM) and an $^{\cdot}NO$-electrode (Ami NO-700; Innovative Instruments, Tampa, FL) in 10 mM potassium phosphate buffer, pH 7.4. The electrode was calibrated every day with $NaNO_2$ standards in 0.1 M H_2SO_4 plus 100 μM potassium iodide. The current difference between base-line buffer signal and the peak following the addition of $NaNO_2$ served for calibration of the instrument. The measurements were performed in stirred glass tubes at 37 °C.

Superoxide ($O_2^{\cdot-}$) Detection by the Cytochrome c Assay—Xanthine oxidase (1 milliunit/ml) plus hypoxanthine (500 μM) in 10 mM potassium phosphate, pH 7.4, were used as a radical generating system. In the presence of test compounds, the reduction of cytochrome *c* (50 μM) was measured by a spectrophotometer at 550 nm in 3-min intervals over a period of 20 min. The samples were incubated in the presence or absence of copper zinc-superoxide dismutase (100 units/ml); the $O_2^{\cdot-}$-dependent part was calculated from the difference between the two corresponding measurements.

Hydroxyl ($^{\cdot}OH$) Radical Generation—Hydroxyl radicals were generated by a combination of ferrous iron (Fe^{2+}) and H_2O_2 and detected by measurement of the formation of chromogens (at 532 nm) that originate from the interaction of deoxyribose degradation products with thiobarbituric acid. One hundred μl of a 150 mM NaCl solution (pH 7.4) were combined freshly with 50 μl of 0.7 mM EDTA, 50 μl of 0.5 mM Fe^{2+} and 100 μl of sample in water. Hydroxyl radical generation was then initiated by the addition of 50 μl of 0.5 mM H_2O_2. The mixture was incubated with additional 100 μl of 5 mM 2-deoxyribose for 20 min at 37 °C under gentle shaking. Then 250 μl of 1% thiobarbituric acid (in 50 mM NaOH) and 250 μl of 2.8% trichloroacetic acid (in water) were added, vortexed thoroughly, shortly centrifuged to remove debris, and read at 532 nm.

HPLC Analysis—Detection of minocycline was performed on a Kontron system (Goebel Analytik, Au/Hallertau, Germany) composed of a model 560 autosampler, a model 520 pump unit, and a model 535 diode array detector set at 350 nm. Separation was carried out on a C8 nucleosil column (250 × 4 mm; 5-μm particle size) from Machery Nagel (Düren, Germany) at room temperature. The mobile phase for minocycline analysis consisted of acetonitrile:methanol:water: trifluoroacetic acid (25: 2: 72.9: 0.1, v/v, pH 1.76). Before use, the mobile phase was degassed and delivered isocratically at a flow rate of 0.8 ml/min at an average pressure of 140 bar. Data

[2] The abbreviations used are: PON, peroxynitrite; ASYN, α-synuclein; DHR 123, dihydrorhodamine 123; AAPH, 2,2-azobis [2-methyl-propionamidine] hydrochloride; 3-NT, 3-nitrotyrosine; LDH, lactate dehydrogenase; ANOVA, analysis of variance; LUHMES, Lund human mesencephalic cells.

analysis was performed with Geminyx II software (Goebel Analytik).

Detection of DNA Oxidation—Oxidative DNA base lesions (8-oxo-2′-deoxyguanosine) were converted into strand breaks by short incubation with formamidopyrimidine-DNA glycolase. The DNA strand breaks were then measured by an automated fluorimetric detection of alkaline DNA unwinding assay described in detail previously (36, 37). The conditions were optimized to allow unwinding of DNA at sites of strand breaks, and the amount of double-stranded DNA was detected by measurement of ethidium bromide incorporation. As a DNA model system, a 14-kbp plasmid (pAcHLT-A-His_6) produced in *Escherichia coli* DH5α cells was treated with minocycline, tetracycline, or gentamicin and 50 μM Sin-1 for 40 min. In each experiment, a full set of controls was run, including calibration controls, and omission of enzyme, challenge, or drug. The data are indicated as fractions of DNA in the unwound state.

Detection of the Common Deletion—Mitochondrial DNA damage following Sin-1 treatment of intact LUHMES cells was assessed by the detection of a 4977-bp deletion, termed common deletion (38). Total DNA of the cell homogenate (including mitochondrial DNA) was collected by extraction using a QIAamp DNA blood mini kit (Qiagen), total DNA content was measured by a Nanodrop 1000 Spectrophotometer (Peqlab, Erlangen, Germany) and adjusted to equal amounts. PCR was performed in 96-well format with a Bio-Rad MyIQ real time PCR apparatus. Amplification was performed using the Platinum® SYBR®Green qPCR SuperMix-UDG kit (Invitrogen). Data analysis was conducted by iCycler software (Bio-Rad), threshold cycles (C_t) were determined for each sample for evaluation. The following primers were used: common deletion forward, 5′-ACC CCC ATA CTC CTT ACA CTA TTC C-3′; common deletion reverse, 5′-AAG GTA TTC CTG CTA ATG CTA GGC T-3′; internal standard forward, 5′-GAT TTG GGT ACC ACC CAA GTA TTG-3′; and internal standard reverse, 5′-AAT ATT CAT GCT GGC TGG CAG TA-3′. After an initial heating step of 1 min at 95 °C, 40 cycles of 15 s at 95 °C (denaturation) and 1 min at 60 °C (annealing and elongation) were run.

Cell Culture—LUHMES cells are conditionally immortalized human fetal ventral mesencephalic neuronal precursor cells that were clonally selected. Differentiated LUHMES show a clear dopaminergic phenotype that was described in detail previously (39, 40). The cells were propagated in Advanced DMEM/F-12 (Invitrogen), 1× N2 supplement (Invitrogen), 2 mM L-glutamine (Invitrogen), and 40 ng/ml recombinant bFGF (R & D Systems, Minneapolis, MN). The differentiation process was initiated by the addition of differentiation medium consisting of advanced DMEM/F-12, 1× N2 supplement, 2 mM L-glutamine, 1 mM dibutyryl-cAMP (Sigma), 1 μg/ml tetracycline (Sigma), and 2 ng/ml recombinant human glial derived neurotrophic factor (GDNF) (R & D Systems). After 2 days, the cells were trypsinized and collected in Advanced DMEM/F-12 medium. The cells were seeded onto 24-well plates at a density of 160,000 cells/cm^2. The differentiation process was continued for an additional 4 days. For the Sin-1/PON treatment experiments, differentiation medium was exchanged to Hanks' balanced salt solution 1 h prior to the experiment and for the decomposition period of 4 h for Sin-1 or Spermine-NONOate to avoid interference with ascorbic acid in the medium. Then Advanced DMEM/F-12 without additions was added for the remaining incubation period of 20 h.

Immunocytochemistry and Analysis of Neurite Degeneration—The cells were fixed with 4% paraformaldehyde for 20 min at room temperature, permeabilized with 0.2% Triton X-100, washed, and blocked with 1% BSA (Calbiochem, San Diego, CA) in PBS for 1 h. For visualization of cell morphology, the cells were stained with a polyclonal anti-β-III-tubulin antibody (Covance, Munich, Germany; 1:1000) in 1% BSA/PBS at 4 °C overnight. After washing, the secondary antibody (anti-mouse-IgG, Alexa 488, Molecular Probes; 1:1000) in 1% BSA/PBS was added for 1 h, the nuclei were stained by Hoechst dye H-33342 (1 μg/ml) for 20 min. For visualization, an Olympus IX 81 microscope (Hamburg, Germany) equipped with a F-view CCD camera was used. For quantitative evaluation of the neurite area, the β-III-tubulin-stained cells were analyzed using an automated microplate-reading microscope (ArrayScan II® HCS Reader; Cellomics, Pittsburgh, PA) equipped with a Hamamatsu ORCA-ER camera (resolution 1024 × 1024; run at 2 × 2 binning) as described previously (39). Briefly, the nuclei were identified as objects according to their intensity, size, area, and shape. A virtual area corresponding to the cell soma was defined around each nucleus. The total β-III-tubulin pixel area per field minus the soma areas in that field was defined as neurite mass.

α-Synuclein Nitration—Purified wild type ASYN (Sigma) (0.5 μg/200 μl of 100 mM potassium phosphate buffer, pH 7.4) was treated in the presence of various concentrations of test compounds with 5 μM PON. One μl of PON (stock 1 mM in 100 mM NaOH) and 1 μl of 100 mM HCl were carefully placed in the inner lid of a reaction tube. After gentle closing, the samples were rapidly vortexed for optimal nitration at constant pH.

α-Synuclein Overexpression—The α-synuclein cDNA was expanded by a C-terminal Myc tag and cloned into the expression vector phsCXW(2), in which the target gene is driven by the cytomegalovirus immediate early promoter. The vector was transfected into HEK 293 cells in 10-cm dishes using the Ca^{2+}-phosphate method. Sixteen hours after transfection, the cells were detached, pooled, and plated in 6-cm dishes at 70% confluency for the incubations. Afterward, all of the homogenates were collected in 300 μl of PBS.

Immunoprecipitation—For the preparation of protein G-antibody complexes, 20 μg of c-Myc monoclonal antibody (Sigma) was added to 200 μl of protein G-4B-Sepharose beads and incubated at room temperature for 2 h. The beads were washed by five centrifugation steps at 12,000 × *g* for 2 min in PBS. Fifty μl of the protein G-antibody complex were mixed with 300 μl of cell homogenate and incubated at 4 °C for at least 24 h under constant shaking. The beads were sedimented and washed with PBS five times at 12,000 × *g* for 2 min. The pellet was finally resuspended in 50 μl of Laemmli buffer, boiled for 5 min, and subjected to Western blot analysis.

Western Blot—ASYN from the nitration experiments was loaded onto a 12% SDS gel (0.1 μg/lane). The proteins were transferred onto nitrocellulose membranes (Amersham Biosciences) and blocked with 5% milk in PBS-Tween (0.1%) for 2 h. Monoclonal antibodies directed against ASYN (1:1000) (32-8100; Zymed Laboratories Inc./Invitrogen) or against 3-nitrotyrosine (3-NT) (1:250) (HBT, HM5001, Uden, The Netherlands) were incubated at 4 °C overnight. The horseradish peroxidase-conjugated secondary antibody (goat anti-mouse IgG; Jackson ImmunoResearch, West Grove, PA) was incubated for 45 min. For quantitative evaluation, luminescence was detected and quantified by a FUSION SL™ system (Peqlab, Erlangen, Germany).

Resazurin Metabolization Assay—Resazurin (Sigma) was added to the cell culture medium in a final concentration of 2.5 μg/ml. Fluorescence was measured in 30-min intervals (λ_{ex} = 530 nm; λ_{em} = 590 nm) over a period of 3 h.

Lactate Dehydrogenase (LDH) Release Assay—LDH activity was detected separately in the supernatant and cell lysate. The cells were lysed in PBS with 0.5% Triton X-100 for 20 min. The percentage of LDH released was calculated as 100 × $LDH_{supernatant}/LDH_{supernatant + lysate}$. For the enzymatic assay, 10 μl of sample was added to 200 μl of reaction buffer containing NADH (100 μM) and sodium pyruvate (600 μM) in sodium phosphate buffer adjusted to pH 7.4 by 40.24 mM K_2HPO_4 and 9.7 mM KH_2PO_4 buffer. Absorption at 340 nm was detected at 37 °C in 1-min intervals over a period of 20 min, and enzyme activity was calculated from the slope.

EPR Measurements—EPR measurements were performed at 20 °C using a MiniScope spectrometer (MS200; Magnettech GmbH) equipped with a variable temperature unit (Temperature Controller TC-H02; Magnettech GmbH). The samples were loaded into glass capillaries (outer diameter, 1 mm) with typical sample volumes of 10 μl. The spectra were obtained in an X-band (9.44 GHz) with a modulation amplitude of 0.6 G, microwave attenuation 10 dB, and a sweep width of 100 G. The signal-to-noise ratio was improved by accumulation of 10 spectra featuring a 60-s scan time each.

Mass Spectroscopic Analysis—α-Synuclein samples were analyzed by reversed phase LC-MS/MS using an LTQ-Orbitrap mass spectrometer (Thermo Fisher) and an Eksigent nano-HPLC. The dimensions of the reversed phase LC column were 5 μm, 200-Å pore size C18 resin in a 75-μm inner diameter × 10-cm-long piece of fused silica capillary (Hypersil Gold C18; New Objective). After sample injection, the column was washed for 5 min with 95% mobile phase A (0.1% formic acid in water) and 5% mobile phase B (0.1% formic acid in acetonitrile), and the peptides were eluted using a linear gradient of 5% mobile phase B to 40% mobile phase B in 65 min and then to 80% B in an additional 5 min at 300 nl/min. The LTQ-Orbitrap mass spectrometer was operated in a data-dependent mode in which each full MS scan (30 000 resolving power) was followed by five MS/MS scans where the five most abundant molecular ions were dynamically selected and fragmented by collision-induced dissociation using a normalized collision energy of 35% in the LTQ ion trap. Dynamic exclusion was allowed. Tandem mass spectra were searched against the Swissprot human protein database using Mascot (Matrix Science) with no enzyme cleavage (because of the use of the unspecific protease pepsin), static cysteine alkylation by iodoacetamide, and variable nitration of Tyr and methionine oxidation.

Minocycline Samples—All of the minocycline samples were analyzed by LC-MS using an Esquire 3000 mass spectrometer (Bruker Daltonics) and an Agilent 1100 micro-HPLC equipped with a Vydac MS C18 reversed phase column (Grace). After sample injection, the column was washed for 5 min with 90% mobile phase A (0.1% formic acid) and 10% mobile phase B (0.1% formic acid in acetonitrile), and minocycline was eluted using 80% mobile phase B with a flow rate of 50 μl/min. The MS data were acquired in a mass range of m/z = 300 to m/z = 1100.

Statistics—The values are expressed as the means ± S.D. ($n \geq 3$). The data were analyzed by one-way ANOVA or Student's t test as appropriate, and the differences were determined by Bonferroni's post hoc test (Prism or Origin software). If not otherwise indicated, the means were considered as statistically significant at $p < 0.05$.

RESULTS

Differential Scavenging of ·NO versus PON by Minocycline—Anti-inflammatory actions of minocycline have been attributed to its ability to limit the production of ·NO. Direct interaction of minocycline with ·NO or PON as a key neurotoxic derivative of ·NO has not been investigated yet. Here, the PON scavenging properties of minocycline were evaluated by an assay in which the test compound competes with the Sin-1-mediated oxidation of DHR 123 to rhodamine (Fig. 1*A*). Sin-1 releases ·NO with a $t_{1/2}$ of ~45 min and concomitantly generates $O_2^{\cdot-}$ in a 1:1 molar ratio. The PON generated under these conditions has a $t_{1/2}$ of ~1–2 s, so that a steady state PON level of ~0.01% of the applied Sin-1 concentration is established. The PON generated by 50 μM Sin-1 (~5 nM steady state PON) led to a strong oxidation of DHR 123 within 15 min. This oxidation was nearly completely blocked by 50 μM minocycline. A half-maximal inhibition was observed at pharmacologically relevant concentrations of ~5 μM, and even 1 μM minocycline led to a significant reduction of ~30% (Fig. 1*A*). To validate the assay, the selective PON scavenger uric acid and the general antioxidant ascorbic acid were used and showed inhibitory effects in the same concentration range as minocycline (not shown).

Interaction of minocycline with ·NO was evaluated by the use of an ·NO-selective electrode. To exclude false-positive signals, the electrode was tested for its reactivity toward PON, $O_2^{\cdot-}$, ·OH-generating systems, and dopamine-semiquinones and revealed no significant increase in signal output even at high concentrations (not shown). As ·NO donor, freshly prepared Spermine-NONOate ($t_{1/2}$ = ~45 min) was added to the system in the presence or absence of minocycline. Even high minocycline concentrations of up to 100 μM did not significantly reduce the ·NO signal. Thus, a direct interaction of ·NO with minocycline can be excluded (Fig. 1*A*). As control, the $O_2^{\cdot-}$-generating system of xanthine oxidase plus its substrate hypoxanthine was added. This lead to a concentration-dependent reduction of the ·NO signal as expected. Under

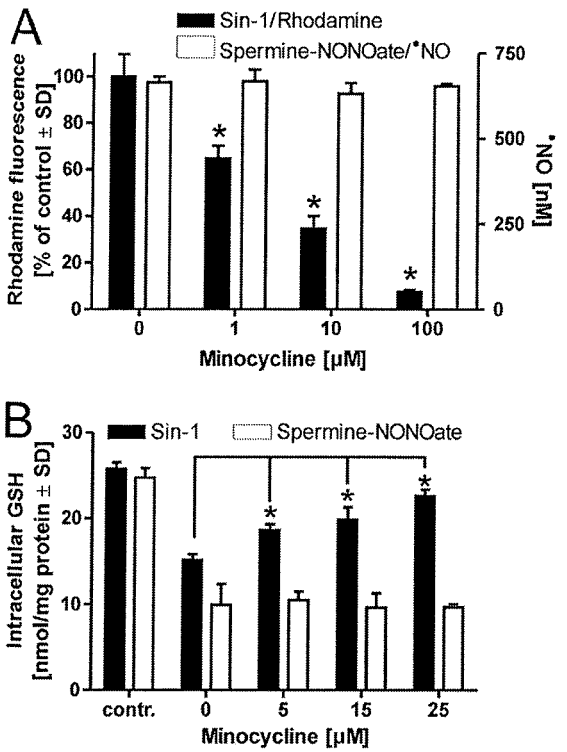

FIGURE 1. **Interaction of minocycline with PON or 'NO.** *A*, minocycline, in the concentrations indicated, was preincubated with the PON donor Sin-1 (50 μM), followed by the addition of DHR 123 (1 μM). Rhodamine generated from DHR 123 was detected in a fluorescence reader. Alternatively, minocycline was pretreated with the 'NO donor Spermine-NONOate (10 μM), and 'NO was measured by a 'NO-selective electrode over a period of 100 s. *B*, human dopaminergic neurons (LUHMES) were exposed to the PON-generating Sin-1 (100 μM) or the 'NO donor Spemine-NONOate (100 μM) in the presence of various concentrations of minocycline or left untreated (control, *contr.*). After 4 h, the incubations were terminated by medium removal and lysis of the cells. The amount of protein and GSH were determined in the lysates. The data are expressed as the means ± S.D. of quadruplicate samples. The statistical significance was determined by one-way ANOVA followed by Bonferroni's post-hoc test. *, $p < 0.05$ *versus* 0 μM minocycline.

these conditions, PON is formed that is not detected by the electrode (not shown). To investigate the cellular relevance of these chemical data, the human dopaminergic cell line LUHMES (39) was chosen.

The levels of intracellular GSH were used as redox readout after treatment with the PON donor Sin-1 or the pure 'NO donor Spermine-NONOate in the presence of various minocycline concentrations. Both treatments lead to a significant decline of reduced GSH within 4 h. Minocycline demonstrated direct antioxidant properties against PON in the 5–25 μM range, whereas no protective effect on 'NO triggered GSH depletion was observed, even at the highest concentrations of minocycline applied (Fig. 1*B*). These initial experiments suggested that minocycline may be a specific PON scavenger rather than a general antioxidant and that this may have relevance in biological systems or diseases.

Specific Peroxynitrite Scavenging by Minocycline—In our initial experiments, PON had been generated by Sin-1. To exclude the possibility that minocycline interfered with the decomposition of this compound and the generation of PON, an alternative system was used. The combination of the 'NO-releasing compound Spermine-NONOate, and the $O_2^{\cdot-}$ generating enzyme xanthine oxidase allows generation of 'NO and $O_2^{\cdot-}$ in an almost 1:1 ratio that is necessary for optimal PON formation. Also in this system, minocycline as well as uric acid and ascorbic acid (not shown) scavenged the generated PON (Fig. 2*A*). As further control, the luminol-derivative L-012 was used as an alternative detection dye instead of DHR 123. L-012 oxidations are relatively specific for PON at the concentrations used here. In combination with Sin-1, minocycline lead to a concentration-dependent decline of L-012 luminescence, whereas tetracycline and gentamicin showed no significant inhibition (Fig. 2*B*). Experiments with uric acid and ascorbic acid demonstrated a concentration-dependent decline in both detection systems (not shown). The significant difference in the PON scavenging capacity of minocycline and tetracycline may be due to the additional dimethylamino substituent in the phenol ring of minocycline compared with tetracycline. To test this assumption, scavenging experiments were performed with 4-dimethylaminophenol in direct comparison with unsubstituted phenol. 4-Dimethylaminophenol, as part of the minocycline structure, exhibited a significant inhibitory impact in the DHR 123/Sin-1 assay system in the low micromolar range, whereas a significant inhibitory impact of phenol (part of tetracycline structure) was only observed at concentrations of 50 μM and higher (Fig. 2*C*). Minocycline was also compared with doxycycline and rifampicin. These drugs were better PON scavengers than tetracycline and were able to prevent the oxidation of the DHR-123 indicator compound by PON. They might offer protection in some *in vivo* models if dosed high enough, but our data indicated that they were still ~100-fold less potent than minocycline (not shown).

Interaction of Minocycline with Other Biologically Relevant Oxygen Radicals—To confirm the interaction of minocycline with authentic PON in an independent test system, EPR spectroscopy was applied to detect the formation of the stable TEMPONE radical generated by the interaction of the spin trap TEMPONE-H with PON. In this system, minocycline reduced TEMPONE formation as efficiently as the established PON scavenger uric acid, whereas tetracycline or gentamicin had no effect at all in this concentration range (Fig. 3*A*).

The primary oxygen radical produced under inflammatory conditions is the superoxide anion ($O_2^{\cdot-}$). To investigate an interaction of $O_2^{\cdot-}$ with minocycline, the radical was enzymatically generated by xanthine oxidase and detected by the cytochrome *c* reduction assay (Fig. 3*B*). To exclude a contribution of other radical species on cytochrome *c* reduction, the experiments were performed in the absence or presence of superoxide dismutase (100 units/ml). The difference between these two conditions was used as readout for the $O_2^{\cdot-}$-specific reduction. Although the control compound ascorbic acid lead to a concentration-dependent decline in $O_2^{\cdot-}$-mediated cytochrome *c* reduction, minocycline had no effect at all in a pharmacologically relevant concentration range (Fig. 3*B*).

Finally, the interaction of the hydroxyl radical ('OH) with minocycline was investigated (Fig. 3*C*). Hydroxyl radicals were generated by a mixture of H_2O_2 and Fe^{2+} according to the Fenton reaction. As readout, deoxyribose was added to the reaction, which forms degradation products that interact

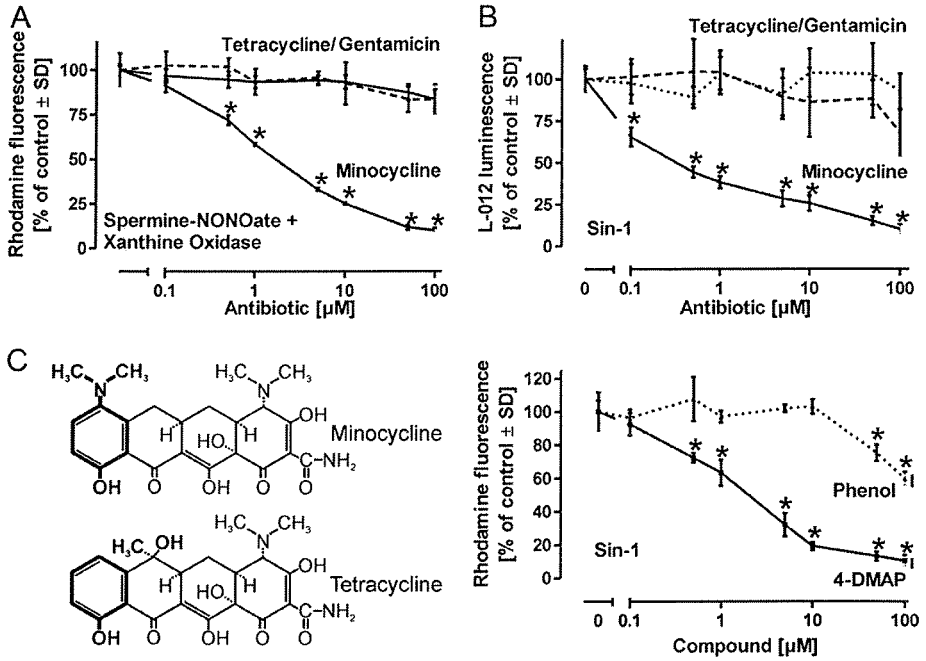

FIGURE 2. **Minocycline as scavenger of peroxynitrite.** *A*, a combination of the 'NO donor Spermine-NONOate (37.5 μM) and the O_2^- generating xanthine oxidase (0.5 milliunit/ml) plus its substrate hypoxanthine (500 μM) was used as a PON generating system in a combination that yields a 1:1 molar ratio of 'NO:O_2^- for maximal PON generation. Minocycline, tetracycline, or gentamicin were added. Five minutes later, DHR 123 (1 μM) was added, and fluorescence was measured after 15 min. *B*, the luminol derivative L-012 (100 μM) was incubated with Sin-1 (50 μM) for 15 min in the dark in the presence of various concentrations of minocycline, tetracycline, or gentamicin, before luminescence was detected. *C*, phenol or 4-dimethylaminophenol (*4-DMAP*) were incubated with the PON generator Sin-1 (50 μM) for 5 min, then DHR 123 (1 μM) was added, and rhodamine fluorescence was detected after 15 min. The statistical significances were determined by one-way ANOVA followed by Bonferroni's post-hoc test. *, $p < 0.05$ *versus* 0 μM minocycline.

with thiobarbituric acid to form an optically detectable chromogen. In the pharmacologically relevant concentration range up to 10 μM, neither minocycline nor tetracycline had an impact on the 'OH-dependent deoxyribose degradation. At concentrations of 50 and 100 μM, a small (10%) but significant inhibition was observed, whereas the known 'OH radical scavenger Me_2SO (positive control) resulted in a significant (20%) inhibition at 5 μM and up to 40% inhibition at 100 μM (Fig. 3*C*). In conclusion, minocycline did not interact with O_2^- or 'NO, whereas it showed weak scavenging of 'OH and potent reaction with PON.

Decomposition of Minocycline by Peroxynitrite—To investigate PON-mediated modifications of the minocycline molecule, the compound was treated with various concentrations of authentic PON and analyzed by HPLC. A concentration-dependent decline in the minocycline peak was observed (Fig. 4*A*). For investigations of the specificity of this reaction, minocycline was treated with PON, the PON generator Sin-1, the O_2^- source KO_2, or the 'OH-generating compound AAPH for 24 h. The remaining minocycline content was quantified by photospectroscopic measurement at 360 nm or by HPLC-based analysis (Fig. 4*B*). Although KO_2 or AAPH treatment hardly lead to a decline, both Sin-1 and PON lead to a significant degradation of minocycline. The HPLC analysis showed no additional peaks as an indicator for a modified minocycline structure. Also, the overall optical spectrum of the final solution from 200 to 600 nm showed no changes (new peaks) apart from the loss of minocycline. These findings may be explained by an opening and disintegration of the polyketide structure. For further analysis, samples of PON-treated minocycline were examined by mass spectrometry. This also demonstrated the disappearance of the minocycline peak (*m/z* 458.5 Da) and the generation of low levels of multiple reaction products (Fig. 4*C*). We next investigated the possibility that not the intact minocycline molecule but rather the decomposition products resulting from an initial interaction with PON may be potent PON scavengers. Minocycline (5 μM) was therefore pretreated with increasing concentrations of authentic PON (Fig. 4*D*). After decomposition of PON, these mixtures were added to a detection system composed of Sin-1 as a source of steady state levels of PON and DHR 123 as readout. The capacity of minocycline to scavenge Sin-1-derived steady state levels of PON was impaired in a concentration-dependent manner when it was pretreated with authentic PON. This strongly suggests that the intact molecule is primarily responsible for the PON scavenging capacity of minocycline (Fig. 4*D*).

Protection of Biomolecules by Minocycline—To investigate potential bio-protective properties of minocycline, plasmid DNA as model system was treated with a fixed concentration of the PON-generating compound Sin-1 (50 μM). Oxidative DNA lesions (8-oxo-deoxyguanosine) were converted into strand breaks by the enzyme formamidopyrimidine-DNA glycolyase. Strand breaks were then detected by an automated fluorescence detection alkaline DNA unwinding assay. Although gentamicin had no effect at all, tetracycline revealed a moderate but significant effect at the highest concentrations of 10 μM, whereas the PON scavenging capacity of minocy-

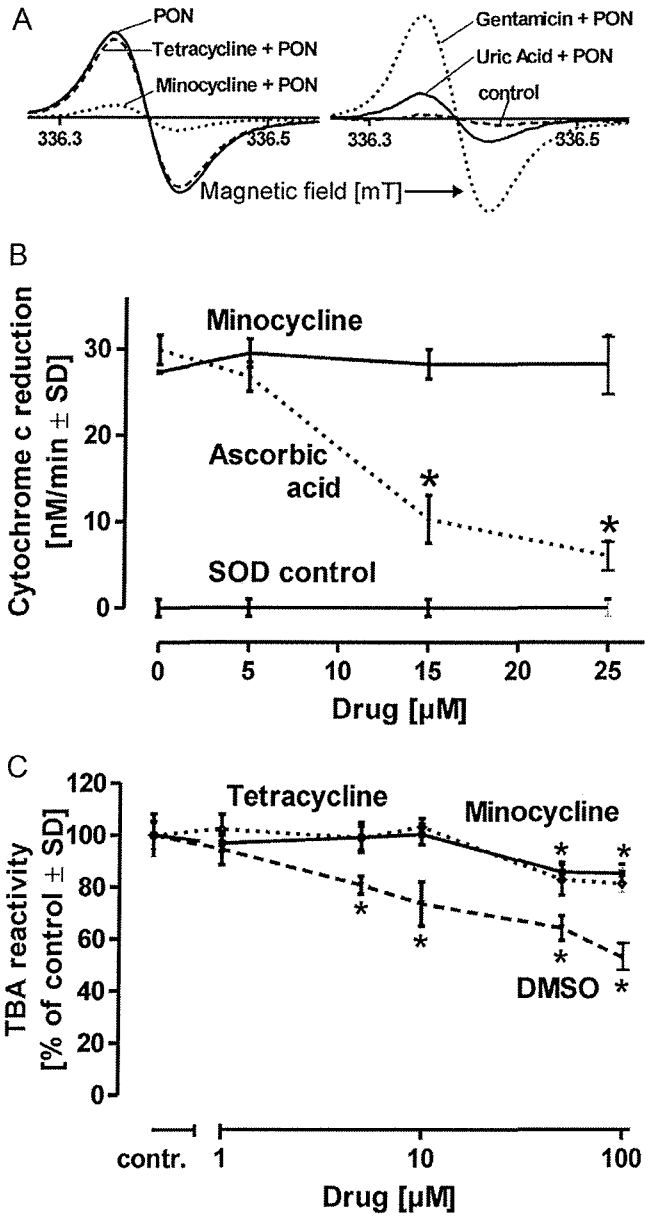

FIGURE 3. **Interaction of minocycline with biologically relevant radical species.** *A*, the spin trap TEMPONE-H (100 μM) was incubated with authentic PON (5 μM) in the presence of 5 μM minocycline, tetracycline, gentamicin, or uric acid to generate the stable TEMPONE-radical detected by EPR spectroscopy. The graphs are representative of three independent experiments. *B*, minocycline or ascorbic acid as control were added to a system of $O_2^{\cdot-}$, generated by xanthine oxidase (0.5 milliunit/ml) and its substrate hypoxanthine (500 μM). $O_2^{\cdot-}$ flux was measured by optical detection of cytochrome *c* reduction (50 μM) over a period of 20 min. *C*, minocycline or tetracycline in the concentrations indicated were incubated with Fe^{2+} and H_2O_2 (50 μM each) as $^{\cdot}OH$ radical generating system. Me_2SO served as positive control. The impact of minocycline, tetracycline, or Me_2SO on $^{\cdot}OH$-dependent 2-deoxyribose degradation was photometrically detected after thiobarbituric acid derivatization. The statistical significance was determined by one-way ANOVA followed by Bonferroni's post-hoc test. *, $p < 0.05$ *versus* 0 μM minocycline.

cline was more pronounced and resulted in an almost complete protection of the DNA from oxidative modifications at concentrations of 5 μM and higher (Fig. 5*A*).

Also in cells, DNA is a target of PON. Mitochondrial DNA is more susceptible to oxidative damage than genomic DNA (41). Such damage often results in the so-called common deletion, *i.e.* a loss of a 5-kbp segment from the mitochondrial genome (38). LUHMES cells were exposed to Sin-1 (500 μM) for 18 h. For the detection of oxidatively modified mitochondrial DNA in living cells, a PCR-based method for the assessment of the common deletion was applied. An increase in the common deletion was detected in the mitochondrial DNA from exposed cells and coincubation with minocycline at concentrations as low as 1 μM reduced this damage (Fig. 5*B*). As a control, decomposed Sin-1 was added and resulted in no common deletions. The addition of minocycline to the LUHMES cultures after total decomposition of Sin-1 (6 h) for an additional 18 h also had no protective effect on the Sin-1-evoked common deletions (not shown).

Among all of the modifications triggered by PON in biological systems, nitration of tyrosine residues is the best characterized and is frequently used as marker for oxidative and nitrative stress. To test whether minocycline can protect tyrosine, the amino acid was treated with PON in the presence of increasing concentrations of antibiotics. Although tetracycline and gentamicin showed no significant impact on 3-NT formation as detected by ELISA, minocycline inhibited the reaction already at submicromolar concentrations (Fig. 5*C*).

Prevention of α-Synuclein Nitration by Minocycline—A disease-relevant example of a protein that can be tyrosine-nitrated is ASYN. Nitrated ASYN was identified as component of the intracellular proteinaceous deposits found in Parkinson disease brains. To investigate the influence of minocycline on ASYN nitration, purified human wild type ASYN was treated with PON in the presence of varying concentrations of antibiotics or uric acid. The nitration of ASYN was completely prevented by minocycline levels of <1 μM. Uric acid was slightly less potent. Tetracycline partially reduced nitration (by 30–40%) in the range of 10–100 μM, whereas gentamicin was without effect (Fig. 6*A*). To investigate the protective impact of minocycline on ASYN nitration in a cellular system, HEK 293 cells stably overexpressing Myc-tagged human wild type ASYN were preincubated with minocycline or the general antioxidant ascorbic acid and nitrated by authentic PON. The protein was recovered by immunoprecipitation against the Myc tag. Western analysis with staining of ASYN and 3-NT revealed that nitration of ASYN was reduced by the presence of minocycline or ascorbic acid (Fig. 6*B*).

On closer examination of the blots stained for ASYN and 3-NT, it became evident that PON treatment resulted in the generation of additional protein bands at higher molecular weights. This strongly indicates the formation of covalently linked ASYN dimers and multimers.

The presence of minocycline or uric acid limited the formation of ASYN dimer and multimers but was not able to completely prevent their generation (Fig. 7*A*). Human ASYN contains four tyrosine residues as potential sites for nitrations. For a more detailed view on the tyrosines involved in the 3-NT formation, purified human wild type ASYN was treated with 5 or 50 μM authentic PON. At both concentrations, mass spectrometric analysis of the digested protein revealed a nitration of the tyrosine residues Tyr^{125}, Tyr^{133}, and Tyr^{136} but not Tyr^{39}. The presence of minocycline completely prevented

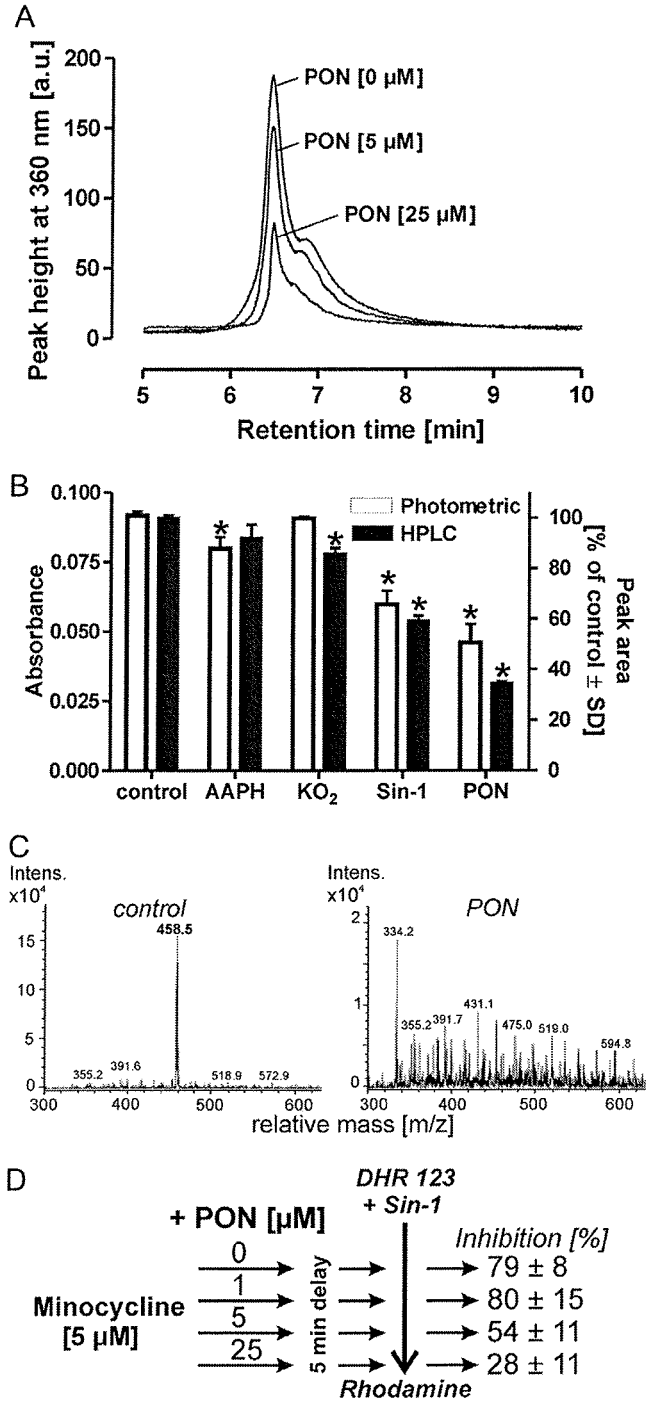

FIGURE 4. **Decomposition of minocycline by PON treatment.** *A*, minocycline (10 µM) was treated with various concentrations of authentic PON. The remaining amount of intact minocycline was quantified by HPLC analysis. *B*, minocycline (10 µM) was treated with the ·OH generator AAPH, KO_2 as a source of $O_2^{\cdot-}$, the PON donor Sin-1, or authentic PON for 24 h. The samples were investigated both by recording of optical spectra between 200 and 600 nm and by HPLC analysis. For quantitative evaluation of the optical spectra, the values at the absorption maximum of minocycline of 360 nm were used. No alternative peak was observed in the optical spectra or in HPLC analysis. *C*, minocycline (100 µM) with or without treatment by authentic PON (100 µM) was subjected to LC-MS/MS mass spectrometric analysis. The minocycline peak at 458.5 Da almost completely vanished, and no dominating alternative peak was observed. *D*, in a first step, minocycline (5 µM) was treated with authentic PON in the concentrations as indicated.

the nitration of all three tyrosines. As an additional post-translational modification, sulfoxidation of methionines Met^{116} and Met^{127} was observed that, in contrast to the nitration of tyrosines, was not prevented by the presence of minocycline (Fig. 7*B*). This suggests that different reactive metabolites formed from peroxynitrous acid may cause different modifications and react differently with minocycline. Fig. 7*B* represents a schematic summary of mass spectrometry data. Detailed information and data can be found in supplemental Fig. S1.

Minocycline Protects Neuronal Cells from PON Treatment—Finally, it was examined whether the direct PON scavenging capacity of minocycline may also be involved in neuroprotection. We used neuronally differentiated LUHMES cells as targets and measured neurite integrity, resazurin reduction, and LDH release as cell death end points (Fig. 8). To exclude that minocycline protected the cells from PON indirectly by blocking death signaling cascades, we made use of the short half-life of authentic PON ($t_{1/2}$ = 1–2 s). When present in the cell culture medium at the time of PON addition (*Mino → PON*), both minocycline and ascorbic acid protected from cell death according to all different end points even when minocycline was washed out 15 min after PON addition (Fig. 8, *A–C*). When minocycline or ascorbic acid was added shortly (5 min) after the addition of PON (*PON → Mino*), no protection was observed. These results strongly suggest that minocycline can protect cells from PON by direct scavenging of this reactive oxygen species.

DISCUSSION

In the present study, we demonstrated that minocycline acts as highly selective scavenger of PON at submicromolar concentrations. This was observed not only in chemically defined assay systems but also in various cellular models, including human neurons. Notably, tetracycline did not show such activity in the low micromolar range, even though it is known that it may scavenge PON in the mM range, similar to most phenolic compounds. No comparative investigations on the interaction of minocycline with biologically relevant radical species have been conducted so far. The high specificity of the antioxidant profile of minocycline is suggested by our findings that the drug interacted neither with ·NO nor with $O_2^{\cdot-}$ or H_2O_2. Interactions with ·OH were observed but were far less pronounced than with PON. The results suggest that a defined target and mechanism of action has been defined for minocycline.

The difference observed for the interaction of minocycline *versus* tetracycline with PON was not found for the ·OH scavenging capacity of the two antibiotics. This may indicate that the interactions of ·OH and PON with minocycline are based on different mechanisms. After exposure of minocycline to PON, we were not able to detect a hydroxylated or nitrated derivative of minocycline or another chemically defined me-

The short $t_{1/2}$ of PON (1–2 s) ensured its complete decomposition within a minute. After 5 min, the pretreated samples were incubated with the PON generator Sin-1 (50 µM) and DHR 123 (1 µM) to test their remaining scavenging capacity. The oxidation of DHR 123 to rhodamine was quantified after 20 min. The statistical significances were determined by one-way ANOVA followed by Bonferroni's post-hoc test. *, $p < 0.05$ *versus* 0 µM minocycline.

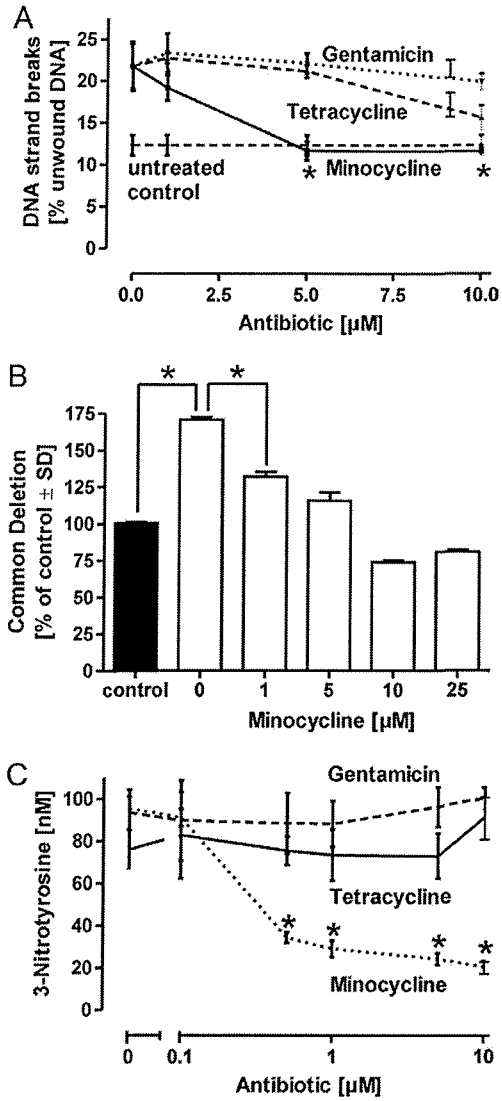

FIGURE 5. **Protection of biological targets by minocycline.** *A*, plasmid DNA was treated with the PON-generating compound Sin-1 (50 μM) in the presence of minocycline, tetracycline, or gentamicin. Following treatment for 4 h, 8-oxo-deoxyguanosine lesions were enzymatically converted into strand breaks that were quantitatively assessed by the fluorimetric detection of alkaline DNA unwinding assay ($n = 4$). *B*, LUHMES cells were treated with the PON donor Sin-1 (250 μM) and different concentrations of minocycline for 18 h. Total DNA was isolated and used as template for PCR amplification. The control value (*black*) indicates cells without Sin-1 treatment. The deletion of a fragment of mitochondrial DNA (common deletion) was evaluated by PCR utilizing settings that allow amplification only when the deletion occurred. Amplification of a stable region of mitochondrial DNA served for standardization. *C*, tyrosine (5 μM) was treated with authentic PON (5 μM) in the presence of various concentrations of minocycline, tetracycline, or gentamicin. Then 3-nitrotyrosine was quantified by ELISA. All of the reactions were carried out in 100 mM potassium phosphate buffer to ensure constant pH. All of the experiments are expressed as the means ± S.D. of quadruplicate samples. The statistical significances were determined by one-way ANOVA followed by Bonferroni's post-hoc test. *, $p < 0.05$ *versus* 0 μM minocycline.

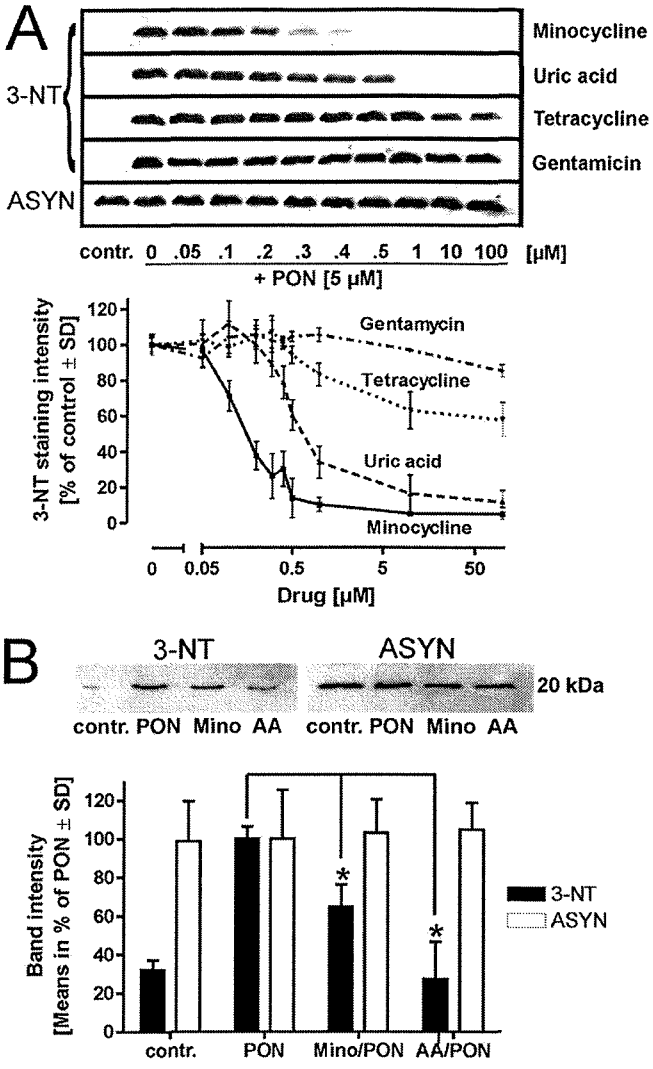

FIGURE 6. **Prevention of ASYN nitration by minocycline.** *A*, purified recombinant human ASYN (0.5 μg/ml) was preincubated for 5 min with minocycline, uric acid, tetracycline, or gentamicin in the concentrations indicated and then treated with PON (5 μM) for 1 min. ASYN nitration was analyzed by Western blot and staining of 3-NT with selective antibodies. Representative blots of three independent experiments are shown. *B*, HEK 293 cells stably overexpressing Myc-tagged human wild type ASYN were pretreated with minocycline (*Mino*, 5 μM), ascorbic acid (*AA*, 50 μM), or left untreated (*contr.*) for 15 min. Then nitration was performed with authentic PON (100 μM). ASYN was recovered from cell homogenates by immunoprecipitation using an anti-Myc antibody and stained for 3-NT and with an anti-ASYN antibody as loading control (*contr.*). The experiments were repeated four times, and band intensities were assessed for quantitative evaluations. The values are the means ± S.D. ($n = 4$). The statistical significances were determined by one-way ANOVA followed by Bonferroni's post-hoc test. *, $p < 0.05$ *versus* 0 μM minocycline.

tabolite. Instead, decomposition of minocycline was observed. Detailed analysis of the degradation products and their impact on biological systems may contribute to the understanding of the side effects of minocycline.

Minocycline demonstrated neuroprotective properties in a variety of chronic neurodegenerative diseases such as Alzheimer disease, Parkinson disease, and amyothrophic lateral sclerosis (6–12). However, no clearly defined molecular target of minocycline action has been described that would explain the wide spectrum of activities of the drug. Our findings that PON is a direct target and chemical interaction partner of minocycline in biological assay systems suggest that this mechanism may be relevant in pathological situations and may contribute to solve the riddle of minocycline action. Neurodegenerative diseases treated with minocycline are all accompanied by an inflammatory activation of glial cells and apoptotic

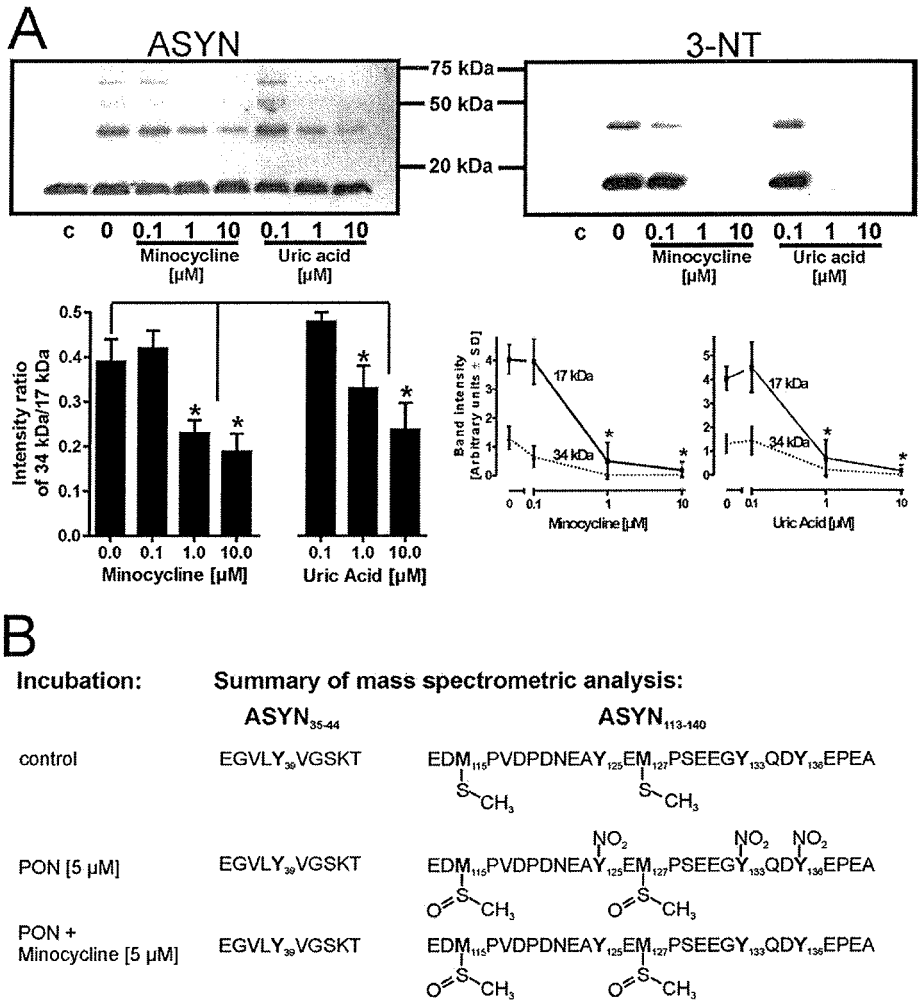

B

Incubation:	Summary of mass spectrometric analysis:	
	$ASYN_{35-44}$	$ASYN_{113-140}$
control	$EGVLY_{39}VGSKT$	$EDM_{115}PVDPDNEAY_{125}EM_{127}PSEEGY_{133}QDY_{136}EPEA$
PON [5 μM]	$EGVLY_{39}VGSKT$	$EDM_{115}PVDPDNEAY_{125}EM_{127}PSEEGY_{133}QDY_{136}EPEA$
PON + Minocycline [5 μM]	$EGVLY_{39}VGSKT$	$EDM_{115}PVDPDNEAY_{125}EM_{127}PSEEGY_{133}QDY_{136}EPEA$

FIGURE 7. **Impact of minocycline on the nitration and formation of ASYN multimers.** *A*, human recombinant ASYN (0.5 μg/ml) was nitrated by authentic PON (5 μM) in the presence or absence of minocycline or uric acid and analyzed by Western blotting. Control values (c) received no minocycline, uric acid, or PON treatment. Staining of ASYN or 3-NT indicated the appearance of additional nitrated ASYN bands following PON treatment with a dominating band at ~34 kDa. The quantitative data were obtained from four independent experiments and expressed as the means ± S.D. *B*, to identify the nitrated tyrosine residues, recombinant human ASYN (0.5 μg in 1 ml) was treated with PON (5 μM) in the presence or absence of minocycline (5 μM). The experiment was repeated until 25 μg of ASYN/condition had been nitrated. Aliquots were then pooled and concentrated to a volume of 500 μl for pepsin digestion and LC-MS/MS analysis. The human 140-amino acid protein ASYN contains four tyrosine residues located at the positions 39, 125, 133, and 136. In addition to tyrosine nitrations, methionine sulfoxidations were observed.

cell death. These processes have been reported to be blocked by minocycline (22, 23). Therefore, the question of an involvement of PON under such conditions arises. In this regard, it is important to be aware of the Janus-faced nature of PON in biological systems, because it can act as a harmful cellular oxidant when generated at high fluxes but importantly also serves as an intracellularly formed signaling molecule affecting several cellular pathways under normal conditions (42).

Minocycline as a Scavenger of Pathologically Relevant PON Concentrations—PON at concentrations sufficient to act as oxidant in the brain primarily occurs following inflammatory activation of glial cells (43). Under such conditions, DNA damage or nitration of proteins can be observed *in vivo* (44, 45). DNA damage was therefore investigated in the present study in a first step by exposure of plasmid DNA to Sin-1-generated fluxes of PON. A concentration-dependent formation of 8-oxo-deoxyguanosine was found and was completely prevented by 5 μM minocycline. This concentration corresponds to the range that can be expected in the brain following repeated standard oral doses of minocycline in clinical studies or animal experiments. The DNA damage was not detected after $^{\bullet}NO$ or $O_2^{\bullet-}$ treatment (not shown). To study the impact of PON on DNA in intact cells, the deletion of a defined segment of mitochondrial DNA was investigated. This study revealed that DNA damage by PON was prevented in a concentration-dependent manner by minocycline. For investigations on the impact of minocycline on the nitration of protein targets, we chose ASYN that is known to be nitrated in patients with Parkinson disease and in animal models of Parkinson disease (46). Here, ASYN was nitrated by PON in a cell-free system as well as in cells, and it was prevented by submicromolar concentrations of minocycline. Although pretreatment with minocycline or uric acid completely prevented nitration of the three C-terminal tyrosines, minocycline did

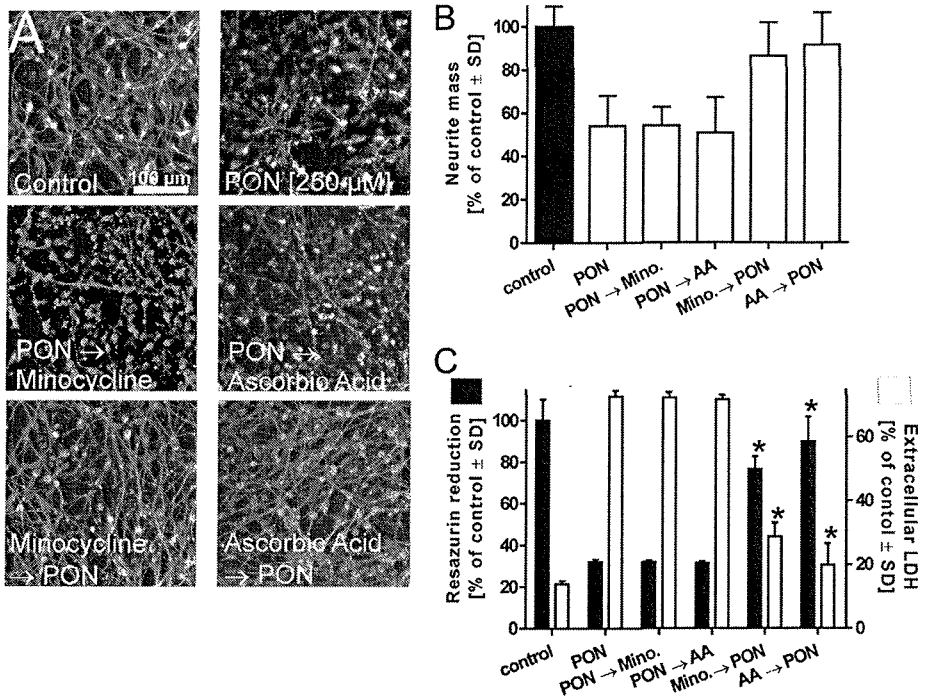

FIGURE 8. **Protection of neuronal cells by direct PON scavenging of minocycline.** *A*, human dopaminergic neurons (LUHMES) were incubated in Hanks' balanced salt solution with minocycline (*Mino*, 10 µM) or ascorbic acid (*AA*, 250 µM) either 5 min before (*Mino → PON*) or 5 min after (*PON → Mino*) the addition of authentic PON (250 µM). The medium was removed from the cells 15 min after treatment, and the cells were then kept in differentiation medium without drugs or additives for additional 18 h. The cells were fixed and stained with a β-III-tubulin antibody for an evaluation of cell morphology. *Scale bar*, 100 µm. *B*, for a quantitative assessment of neurite mass, cells were fixed, stained for β-III-tubulin and for nuclear DNA (Hoechst H-33342), and analyzed by an automated microscope system with imaging algorithms allowing a discrimination between cell bodies and cell extensions. *C*, cell viability was assessed by the resazurin reduction and LDH release assays. The data are the means ± S.D. of quadruplicates. The statistical significance was determined by one-way ANOVA followed by Bonferroni's post-hoc test. *, $p < 0.05$ *versus* 0 µM minocycline.

not prevent the oxidation of the two methionine residues present in ASYN. Nitration of tyrosine primarily occurs via attack by the $^{\bullet}NO_2$ radical that originates from the decomposition of peroxynitrous acid (47), and minocycline may directly interact with this specific radical. Our findings are consistent with the view that methionine oxidation is mediated by a different radical species. Others reported that $^{\bullet}OH$, as another degradation product of peroxynitrous acid, plays no significant role in methionine oxidation (30). Instead, a two electron oxidation by an interaction with the electrophilic nitrogen of peroxynitrous acid and the sulfur atom of methionine has been proposed and thus could be responsible for the observations made in our study (48, 49). The neutralization of $^{\bullet}OH$ may be relevant in pathological situations favoring the Fenton reaction, as for example in the iron-rich substantia nigra in Parkinson disease. The effect of $^{\bullet}OH$ scavenging would become pharmacologically relevant only at higher concentrations of minocycline (>10 µM), that are likely to be reached in several animal studies described in the literature (8).

Minocycline as Scavenger of Physiological PON Concentrations—Pathologically high concentrations of PON are usually found under conditions when the inducible isoform of nitric-oxide synthase (NOS-2) is the source of $^{\bullet}NO$. When minocycline is considered as a scavenger of PON in its role as signaling molecule, the question arises regarding how $^{\bullet}NO$ is generated in the absence of NOS-2 expression. The significance of the constitutively expressed brain isoform NOS-1 has been underestimated for a long time, although it has been known that NOS-1 contributes to brain damage associated with DNA lesions or PARP activation (45, 50, 51). Recent findings indicated nitration of proteins in activated cells in the absence of inducible NOS-2 (52). NOS-1 activity is mainly regulated by levels of cytosolic free Ca^{2+}, and hence, Ca^{2+} becomes a key regulator in the endogenous formation of PON. Glutamate excitotoxicity represents a classical model of elevated cytosolic Ca^{2+} levels (53), and in such models, minocycline concentrations in the low nanomolar range have been reported to be neuroprotective (11). Similar observations were made in 1-Methyl-4-phenyl-1,2,3,6-tetrahydropyridine (MPTP)/1-Methyl-4-phenylpyridinium (MPP^+) models that are also characterized by disturbed cellular Ca^{2+} homeostasis (54). Further indirect evidence for a role of PON scavenging by minocycline comes from experiments in which cerebellar granule cells were treated with subtoxic concentrations of an $^{\bullet}NO$ donor and MPP^+ that together allow formation of PON (8). In all of these models, minocycline demonstrated neuroprotective effects, and we suggest that at least some of its protective properties may originate from a direct scavenging of the intracellular signaling molecule PON.

In chronic neurodegenerative disorders, PON signaling may be involved in the assembly of the mitochondrial permeability transition pore complex, leading to cytochrome *c* release (15). Moreover, PON is pivotally involved in the activation of signaling cascades such as p38 MAPK or NF-κB (26,

32, 33). It might therefore be speculated that scavenging of PON contributes to the observations on an inhibition of cytochrome *c* release as well as the repeatedly described inhibitory effect on the p38 signaling cascade and on induction of pro-inflammatory enzymes such as NOS-2 or COX-2 in glial cells.

In this work, we have demonstrated that minocycline is a selective and potent scavenger of PON. The compound protected cells from exogenously added PON. Under such conditions that, for example, reflect the situation of inflammatory glia activation and its impact on neurons in the brain, relatively high concentrations of the antibiotic in the micromolar range are required to scavenge PON sufficiently fast to achieve protection. In contrast, considering the role of endogenous low levels of PON as intracellular signaling molecules under chronic pathological conditions, and the excellent penetration of biological membranes by minocycline, nanomolar concentrations might be sufficient to interrupt chronic processes that would ultimately lead to cell death.

Acknowledgment—We are particularly thankful to Prof. V. Ullrich for fruitful discussions and careful reading of the manuscript.

REFERENCES

1. Kelly, R. G., and Kanegis, L. A. (1967) *Toxicol. Appl. Pharmacol.* **11,** 171–183
2. Goulden, V., Glass, D., and Cunliffe, W. J. (1996) *Br. J. Dermatol.* **134,** 693–695
3. Saivin, S., and Houin, G. (1988) *Clin. Pharmacokinet.* **15,** 355–366
4. Yong, V. W., Wells, J., Giuliani, F., Casha, S., Power, C., and Metz, L. M. (2004) *Lancet Neurol.* **3,** 744–751
5. Kim, H. S., and Suh, Y. H. (2009) *Behav. Brain Res.* **196,** 168–179
6. Wang, C. X., Yang, T., Noor, R., and Shuaib, A. (2002) *BMC Neurol.* **2,** 2
7. Kriz, J., Nguyen, M. D., and Julien, J. P. (2002) *Neurobiol. Dis.* **10,** 268–278
8. Du, Y., Ma, Z., Lin, S., Dodel, R. C., Gao, F., Bales, K. R., Triarhou, L. C., Chernet, E., Perry, K. W., Nelson, D. L., Luecke, S., Phebus, L. A., Bymaster, F. P., and Paul, S. M. (2001) *Proc. Natl. Acad. Sci. U.S.A.* **98,** 14669–14674
9. Familian, A., Boshuizen, R. S., Eikelenboom, P., and Veerhuis, R. (2006) *Glia* **53,** 233–240
10. Chen, M., Ona, V. O., Li, M., Ferrante, R. J., Fink, K. B., Zhu, S., Bian, J., Guo, L., Farrell, L. A., Hersch, S. M., Hobbs, W., Vonsattel, J. P., Cha, J. H., and Friedlander, R. M. (2000) *Nat. Med.* **6,** 797–801
11. Yrjänheikki, J., Tikka, T., Keinänen, R., Goldsteins, G., Chan, P. H., and Koistinaho, J. (1999) *Proc. Natl. Acad. Sci. U.S.A.* **96,** 13496–13500
12. Tikka, T. M., and Koistinaho, J. E. (2001) *J. Immunol.* **166,** 7527–7533
13. Brundula, V., Rewcastle, N. B., Metz, L. M., Bernard, C. C., and Yong, V. W. (2002) *Brain* **125,** 1297–1308
14. Gieseler, A., Schultze, A. T., Kupsch, K., Haroon, M. F., Wolf, G., Siemen, D., and Kreutzmann, P. (2009) *Biochem. Pharmacol.* **77,** 888–896
15. Wilkins, A., Nikodemova, M., Compston, A., and Duncan, I. (2004) *Neuron Glia Biol.* **1,** 297–305
16. Yrjänheikki, J., Keinänen, R., Pellikka, M., Hökfelt, T., and Koistinaho, J. (1998) *Proc. Natl. Acad. Sci. U.S.A.* **95,** 15769–15774
17. Choi, S. H., Lee, D. Y., Chung, E. S., Hong, Y. B., Kim, S. U., and Jin, B. K. (2005) *J. Neurochem.* **95,** 1755–1765
18. Tomás-Camardiel, M., Rite, I., Herrera, A. J., de Pablos, R. M., Cano, J., Machado, A., and Venero, J. L. (2004) *Neurobiol. Dis.* **16,** 190–201
19. Cho, Y., Son, H. J., Kim, E. M., Choi, J. H., Kim, S. T., Ji, I. J., Choi, D. H., Joh, T. H., Kim, Y. S., and Hwang, O. (2009) *Neurotox. Res.* **16,** 361–371
20. Agostini, S., Eutamene, H., Cartier, C., Broccardo, M., Improta, G., Houdeau, E., Petrella, C., Ferrier, L., Theodorou, V., and Bueno, L. (2010) *Gastroenterology* **139,** 553–563
21. Bradesi, S., Svensson, C. I., Steinauer, J., Pothoulakis, C., Yaksh, T. L., and Mayer, E. A. (2009) *Gastroenterology* **136,** 1339–1348
22. Tikka, T., Fiebich, B. L., Goldsteins, G., Keinanen, R., and Koistinaho, J. (2001) *J. Neurosci.* **21,** 2580–2588
23. Filipovic, R., and Zecevic, N. (2008) *Exp. Neurol.* **211,** 41–51
24. Kraus, R. L., Pasieczny, R., Lariosa-Willingham, K., Turner, M. S., Jiang, A., and Trauger, J. W. (2005) *J. Neurochem.* **94,** 819–827
25. Zhu, S., Stavrovskaya, I. G., Drozda, M., Kim, B. Y., Ona, V., Li, M., Sarang, S., Liu, A. S., Hartley, D. M., Wu, D. C., Gullans, S., Ferrante, R. J., Przedborski, S., Kristal, B. S., and Friedlander, R. M. (2002) *Nature* **417,** 74–78
26. Lin, S., Zhang, Y., Dodel, R., Farlow, M. R., Paul, S. M., and Du, Y. (2001) *Neurosci. Lett.* **315,** 61–64
27. Machado, L. S., Kozak, A., Ergul, A., Hess, D. C., Borlongan, C. V., and Fagan, S. C. (2006) *BMC Neurosci.* **7,** 56
28. Schildknecht, S., Daiber, A., Ghisla, S., Cohen, R. A., and Bachschmid, M. M. (2008) *FASEB J.* **22,** 215–224
29. Falsig, J., van Beek, J., Hermann, C., and Leist, M. (2008) *J. Neurosci. Res.* **86,** 1434–1447
30. Pryor, W. A., Jin, X., and Squadrito, G. L. (1994) *Proc. Natl. Acad. Sci. U.S.A.* **91,** 11173–11177
31. Beckman, J. S. (1996) *Chem. Res. Toxicol.* **9,** 836–844
32. Yakovlev, V. A., Barani, I. J., Rabender, C. S., Black, S. M., Leach, J. K., Graves, P. R., Kellogg, G. E., and Mikkelsen, R. B. (2007) *Biochemistry* **46,** 11671–11683
33. Jope, R. S., Zhang, L., and Song, L. (2000) *Arch. Biochem. Biophys.* **376,** 365–370
34. Hodara, R., Norris, E. H., Giasson, B. I., Mishizen-Eberz, A. J., Lynch, D. R., Lee, V. M., and Ischiropoulos, H. (2004) *J. Biol. Chem.* **279,** 47746–47753
35. Whiteman, M., and Halliwell, B. (1997) *Free Radic. Res.* **26,** 49–56
36. Moreno-Villanueva, M., Pfeiffer, R., Sindlinger, T., Leake, A., Müller, M., Kirkwood, T. B., and Bürkle, A. (2009) *BMC Biotechnol.* **9,** 39
37. Wenzel, P., Schuhmacher, S., Kienhöfer, J., Müller, J., Hortmann, M., Oelze, M., Schulz, E., Treiber, N., Kawamoto, T., Scharffetter-Kochanek, K., Münzel, T., Bürkle, A., Bachschmid, M. M., and Daiber, A. (2008) *Cardiovasc. Res.* **80,** 280–289
38. Koch, H., Wittern, K. P., and Bergemann, J. (2001) *J. Invest. Dermatol.* **117,** 892–897
39. Schildknecht, S., Pöltl, D., Nagel, D. M., Matt, F., Scholz, D., Lotharius, J., Schmieg, N., Salvo-Vargas, A., and Leist, M. (2009) *Toxicol. Appl. Pharmacol.* **241,** 23–35
40. Lotharius, J., Falsig, J., van Beek, J., Payne, S., Dringen, R., Brundin, P., and Leist, M. (2005) *J. Neurosci.* **25,** 6329–6342
41. Yakes, F. M., and Van Houten, B. (1997) *Proc. Natl. Acad. Sci. U.S.A.* **94,** 514–519
42. Schildknecht, S., and Ullrich, V. (2009) *Arch. Biochem. Biophys.* **484,** 183–189
43. Arimoto, T., and Bing, G. (2003) *Neurobiol. Dis.* **12,** 35–45
44. Iravani, M. M., Kashefi, K., Mander, P., Rose, S., and Jenner, P. (2002) *Neuroscience* **110,** 49–58
45. Su, J. H., Deng, G., and Cotman, C. W. (1997) *Brain Res.* **774,** 193–199
46. Giasson, B. I., Duda, J. E., Murray, I. V., Chen, Q., Souza, J. M., Hurtig, H. I., Ischiropoulos, H., Trojanowski, J. Q., and Lee, V. M. (2000) *Science* **290,** 985–989
47. van der Vliet, A., Eiserich, J. P., O'Neill, C. A., Halliwell, B., and Cross, C. E. (1995) *Arch. Biochem. Biophys.* **319,** 341–349
48. Perrin, D., and Koppenol, W. H. (2000) *Arch. Biochem. Biophys.* **377,** 266–272
49. Schöneich, C. (2005) *Biochim. Biophys. Acta* **1703,** 111–119
50. Schulz, J. B., Matthews, R. T., Klockgether, T., Dichgans, J., and Beal, M. F. (1997) *Mol. Cell. Biochem.* **174,** 193–197
51. Leist, M., and Nicotera, P. (1998) *Exp. Cell Res.* **239,** 183–201
52. Imam, S. Z., el-Yazal, J., Newport, G. D., Itzhak, Y., Cadet, J. L., Slikker, W., Jr., and Ali, S. F. (2001) *Ann. N.Y. Acad. Sci.* **939,** 366–380
53. Nicotera, P., Leist, M., and Manzo, L. (1999) *Trends Pharmacol. Sci.* **20,** 46–51
54. Kass, G. E., Wright, J. M., Nicotera, P., and Orrenius, S. (1988) *Arch. Biochem. Biophys.* **260,** 789–797